



HAL
open science

Hydrological control, fractionation, and fluxes of dissolved rare earth elements in the lower Orinoco River, Venezuela

Abrahan Mora, Cristina Moreau, Jean-Sébastien Moquet, Marjorie Gallay, Jürgen Mahlknecht, Alain Laraque

► **To cite this version:**

Abrahan Mora, Cristina Moreau, Jean-Sébastien Moquet, Marjorie Gallay, Jürgen Mahlknecht, et al.. Hydrological control, fractionation, and fluxes of dissolved rare earth elements in the lower Orinoco River, Venezuela. *Applied Geochemistry*, 2020, 112, pp.104462. 10.1016/j.apgeochem.2019.104462 . insu-02937185

HAL Id: insu-02937185

<https://insu.hal.science/insu-02937185>

Submitted on 12 Sep 2020

HAL is a multi-disciplinary open access archive for the deposit and dissemination of scientific research documents, whether they are published or not. The documents may come from teaching and research institutions in France or abroad, or from public or private research centers.

L'archive ouverte pluridisciplinaire **HAL**, est destinée au dépôt et à la diffusion de documents scientifiques de niveau recherche, publiés ou non, émanant des établissements d'enseignement et de recherche français ou étrangers, des laboratoires publics ou privés.



Distributed under a Creative Commons Attribution - NoDerivatives 4.0 International License



Hydrological control, fractionation, and fluxes of dissolved rare earth elements in the lower Orinoco River, Venezuela

Abrahan Mora^{a,*}, Cristina Moreau^a, Jean-Sébastien Moquet^b, Marjorie Gallay^{c,d}, Jürgen Mahlknecht^a, Alain Laraque^e

^a Centro del Agua para América Latina y el Caribe, Escuela de Ingeniería y Ciencias, Tecnológico de Monterrey, Monterrey, Mexico

^b Institut de Physique du Globe de Paris, Sorbonne Paris Cité, Université Paris Diderot, UMR 7154 CNRS, F-75005, Paris, France

^c Office de l'Eau de Guyane, Cayenne, France

^d IRD/GET – UMR 5563, UR 234, Toulouse, France

^e GET, UMR CNRS/IRD/UPS, UMR 5563 du CNRS, UR 234 de l'IRD, OMP 14 Avenue Edouard Belin, 31400, Toulouse, France

ARTICLE INFO

Editorial handling by Dr T Pichler

Keywords:

Rare earth elements
Orinoco River
Hydrological variation
Atlantic ocean
Nd fluxes

ABSTRACT

The monthly variation of dissolved rare earth elements (REEs) was assessed in the lower Orinoco River during a two year period (2007–2008) to determine the seasonal variability of REE concentrations, to identify the variables that exert the main control in their concentrations and fractionation, and to quantify the annual fluxes of dissolved REEs to the Orinoco estuary. Overall, the abundance of dissolved REEs is dominated by hydrological variations in the water discharge, wherein the lowest concentrations and greater fractionation occur during low water-discharge periods. The pH and Al- and Fe-mineral colloids are identified as the main variables that control both the abundance and fractionation of dissolved REEs. An enrichment of heavy REEs (HREEs) relative to light REEs (LREEs) occurs at circumneutral and alkaline pH values. However, the logarithmic relationships between the Yb_{UCC}/Nd_{UCC} ratios and Al and Fe concentrations indicate that Al- and Fe-mineral colloids are responsible for the progressive enrichment of LREEs relative to HREEs under acidic conditions. The Ce and Eu anomalies are also dominated by variations in the water discharge. Negative Ce-anomalies are observed during low flow periods. This is probably due to the signature of the Andean host rocks and/or the oxidation and co-precipitation of Ce (III) to CeO_2 at alkaline pH. However, the lesser Ce fractionated values during flood/high-water periods may indicate less oxidized/more reduced source conditions during these periods. Conversely, positive Eu anomalies are observed during low-water periods because of the preferential weathering of plagioclase in shield terranes and Eu-bearing minerals in the Andes. The fluxes of dissolved REEs from the lower Orinoco River to the Orinoco estuary display strong inter-annual variations, which range from 45.6% for Lu to 56.5% for Gd. These results highlight the importance of performing monthly and inter-annual REE time series in order to develop a more precise quantification of the annual REE fluxes from large rivers to the oceans.

1. Introduction

The biogeochemical processes occurring at the scale of the main intertropical basins are of high importance to oceanic biogeochemical cycles. Global rivers annually discharge $\sim 35\,000\text{ km}^3$ of freshwater and export approximately $3.9 \times 10^9\text{ t}$ of dissolved load, $18 \times 10^9\text{ t}$ of sediment, and $1.06 \times 10^9\text{ t}$ of carbon to the oceans (Li et al., 2017; Milliman, 2001). However, these estimates are not well constrained for rare earth elements (REEs), which are part of these biogeochemical cycles and are

particularly relevant to estuarine, coastal, and ocean ecosystems (Eldersfield et al., 1990; Haley et al., 2017).

The REE group is composed of 14 chemical elements (from La to Lu). These have been used for paleo-environmental reconstruction (Sheng et al., 2018) and for investigating a broad range of geochemical processes including ocean circulation (Laukert et al., 2017), weathering, erosion and riverine transport (Gaillardet et al., 1997; Su et al., 2017), provenance of sediments and sands (Liu and Yang, 2018), and the tectonic evolution of regional orogenic belts (Liu et al., 2018) and the

* Corresponding author. Centro del Agua para América Latina y el Caribe, Escuela de Ingeniería y Ciencias, Tecnológico de Monterrey, Av. Eugenio Garza Sada Sur N° 2501, CP 64849, Monterrey, Nuevo León, Mexico.

E-mail address: abrahanmora@tec.mx (A. Mora).

<https://doi.org/10.1016/j.apgeochem.2019.104462>

Received 29 January 2019; Received in revised form 31 October 2019; Accepted 1 November 2019

Available online 3 November 2019

0883-2927/© 2019 The Authors.

Published by Elsevier Ltd.

This is an open access article under the CC BY-NC-ND license

(<http://creativecommons.org/licenses/by-nc-nd/4.0/>).

continental crust (Taylor et al., 1981). The REEs are classified into two categories: light REEs (LREEs, from La to Eu) and heavy REEs (HREEs, from Gd to Lu). However, some researchers add a third category referred to as the middle REEs (from Nd to Gd) (Sholkovitz, 1995).

The abundance patterns of REEs in the dissolved and suspended material of river water provide insights into both their seawater cycle and their abundances in the continental crust (Goldstein and Jacobsen, 1988). However, the natural signature of REEs may become altered because of the increasing anthropogenic activities in watersheds (Song et al., 2017). Similarly, the abundance and fractionation of dissolved REEs in pristine or natural waters may also depend on certain intrinsic characteristics of rivers including salinity, pH, redox potential, flow conditions, microorganism activity, and variations in atmospheric precipitation (Deberdt et al., 2002; Cidu and Biddau, 2007; García et al., 2007; Xu and Han, 2009; Radomskaya et al., 2017; Sklyarova et al., 2017).

Over the past four decades, several studies have been carried out to investigate the concentrations and fractionation patterns of REEs in rivers (Goldstein and Jacobsen, 1988; Elderfield et al., 1990; Sholkovitz, 1995; Zhang, 1998; Gerard et al., 2003; Rengarajan and Sarin, 2004; Uchida et al., 2006; Ryu et al., 2007; Sultan and Shazili, 2009; Piper and Bau, 2013; Duvert et al., 2015; Radomskaya et al., 2017; Sklyarova et al., 2017). In addition, a few investigations have been performed to assess the temporal variability of REEs in globally significant large rivers, e.g., the Xijiang River (China), Mississippi River (USA), and Amazon River and its major tributaries (Shiller, 2002; Barroux et al., 2006; Xu and Han, 2009). Nevertheless, the geochemistry and temporal variation of dissolved REEs in the Orinoco River have not been evaluated. Only a few studies based on a sampling campaign have measured the concentrations of REEs in this large tropical river. Therefore, given the lack of information on the dissolved-REE dynamics in the Orinoco River, this study addresses the following questions: i) Are dissolved REEs driven by the hydrological variations (seasonal variations in water discharge) in the Orinoco River? ii) Which processes mainly control the concentration and fractionation of dissolved REEs in the Orinoco River? iii) What is the quantity of dissolved REEs exported annually from the Orinoco River to the Orinoco estuary? Because REE dynamics can provide important information on weathering and the geochemical processes occurring in continents and oceans, we provide a comparative analysis of the dissolved REE composition of the Orinoco River over a 24 month period, from January 2007 to December 2008. We carried out a systematic investigation that focused on two objectives, (i) to evaluate the temporal variability of dissolved REE concentrations in the lower Orinoco River and to identify the processes controlling their dynamics, and (ii) to quantify the annual fluxes of dissolved REEs from the Orinoco River to the Orinoco Estuary.

2. Environmental and hydrological settings

The Orinoco River is the second largest river in South America and is ranked third in the world with respect to water discharge to the oceans. Its basin covers an area of 990 000 km² (Berner and Berner, 1987), 70% of which is in Venezuela and 30% is in Colombia (Lewis and Saunders, 1989). The channel length of the Orinoco River is ~2140 km (Silva León, 2005), whereas the estimated mean annual discharge at the river mouth is ~37 600 m³ s⁻¹ (Laraque et al., 2013).

The oscillation of the intertropical convergence zone (ITCZ) determines the pluvial regime and climate of the Orinoco basin, and produces a seasonally tropical climate that comprises two seasons: a rainy season (May to November) and a dry season (December to April). These distinct seasons cause seasonally variable discharges to the lower Orinoco River that differ by a factor higher than 10 over the year (Weibe-zahn, 1990). The maximum flows occur between July and September, and the flood peak is commonly recorded in late August or early September. Lower flows occur between February and April, and the minimum flow is observed during late March to early April (Warne et al.,

2002). With regard to the sedimentary pattern, the concentrations of suspended material transported by the Orinoco River display a strong seasonal variation between 20 and 180 mg L⁻¹ over the hydrological year. Here, the minimum suspended solid concentrations occur during the lowest and highest water discharge periods, and the maximum concentrations occur during periods of rising (May and June) and falling (November) water levels (Laraque et al., 2013).

The Orinoco River receives inputs from numerous tributaries. These tributaries exhibit different physicochemical characteristics that depend largely on the lithology and geomorphology of the drainage basin. The drainage basin comprises three major physiographic zones: the Andes, Llanos, and Guayana Shield. The Andes and the Caribbean coastal ranges are active mountain ranges located to the west and north of the basin, respectively. They contain a mixture of carbonate, silicate, and evaporite rocks. In these regions, physical erosion occurs at a faster rate than chemical weathering (reaction-limited weathering regime), and rivers have high pH, elevated concentrations of major ions (Na⁺, K⁺, Ca²⁺, Mg²⁺, SO₄²⁻, HCO₃⁻, and Cl⁻), and transport high loads of immature suspended sediments (whitewater rivers) (Stallard et al., 1991; Mora et al., 2010). The Llanos or lowland alluvial floodplains comprise approximately 50% of the basin and are located to the northwest between the mountain ranges and the Orinoco River channel. This area is composed of silico-clastic sedimentary rocks/deposits mainly inherited from the erosional processes of the Andes (western and central Llanos) and Guayana Shield (eastern Llanos). The rivers that originate entirely from the Llanos (clearwater rivers) have very low concentrations of dissolved cations because the sedimentary material is more resistant to weathering than the Andean lithologies. The Precambrian Guayana Shield is a highly eroded crystalline bedrock zone dominated by granites with high contents of SiO₂, K-feldspars, plagioclases, and quartz arenites. Owing to the lithology of the area, the weathering and erosional processes in these Precambrian terranes are slow. In fact, the rate of chemical weathering is faster than that of mechanical erosion (a transport-limited weathering regime), and rivers transport low quantities of suspended material that mainly comprises kaolinite and gibbsite (Stallard et al., 1991). Therefore, rivers flowing from the Guayana Shield are between blackwater and clearwater rivers due to the low pH, low concentrations of dissolved major ions (because of the slow weathering process), and relative abundance of humic and fulvic substances. In general, the water sources of the Orinoco are divided equally between the Guayana Shield (50%) and the combined Llanos and Andes regions (50%). Conversely, more than 95% of the suspended load is exclusively derived from the Andes and Llanos, and a lesser proportion is derived from the Paleoproterozoic terranes of the Guayana Shield (Meade et al., 1990).

The mean annual temperature in the basin is ~26 °C, and the mean annual precipitation and runoff are 1900 mm and 1185 mm, respectively, which is an intrinsic characteristic of warm and humid tropical climates. Although the oscillation of the ITCZ controls the climate system in the Orinoco basin, each physiographic region varies in vegetation type and climate (Weibe-zahn, 1990). For example, the mean temperature in the Andes is highly dependent on the altitude, whereas very high rainfall (up to 5000 mm per year) occurs in the south of the basin at the headwater of the Guayana Shield.

3. Materials and methods

3.1. Sampling

Water samples were collected monthly from a small boat in the middle of the Orinoco River channel at the gauging station of Ciudad Bolívar (8°08'38"N, 63°36'28"W) between January 2007 and December 2008 (Fig. 1). Ciudad Bolívar is the principal hydrological gauging station in the Orinoco basin, and daily water levels and discharges of the Orinoco River have been recorded since 1926. The lateral chemical asymmetry reported for the Orinoco River disappears at this gauging

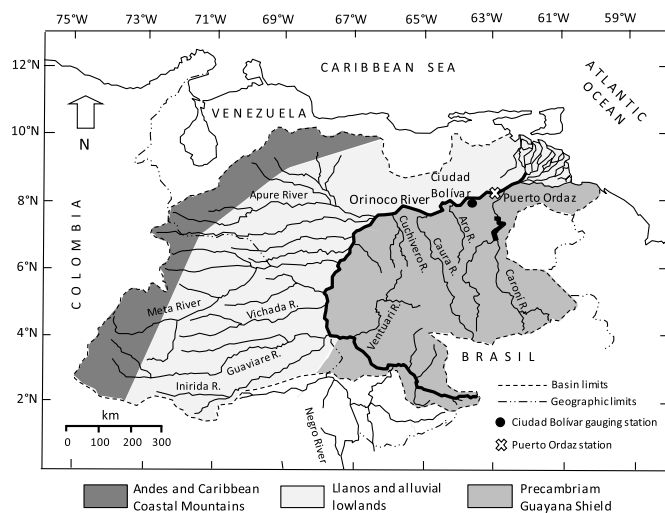


Fig. 1. Map of the Orinoco River basin showing the major tributaries, the three major physiographic zones and the location of Ciudad Bolívar gauging station and Puerto Ordaz (Adapted from Warne et al., 2002).

station because of the considerable shrinkage of the main channel and the presence of bedrock outcrops that homogenize the Orinoco waters (Laraque et al., 2013).

All the water samples were collected from 50 cm below the surface in polyethylene bottles, which were pre-washed with nitric acid and deionized water. During collection, the polyethylene bottles were rinsed three times with river water and then filled completely to avoid any remaining space inside the bottles. After sampling, the water samples were placed in a cooler with ice and transported immediately to the laboratory of Universidad Nacional Experimental de Guayana (UNEG) in Puerto Ordaz (80 km downstream of Ciudad Bolívar) for filtration and preservation processing. The samples were filtered approximately 2 h after collection through frontal filtration using 0.22 μm pore-size polyethylsulfone (PES) Millipore® membranes. This fraction includes organic and inorganic Al- and Fe-colloids and the fraction of REEs that is complexed and/or scavenged with organic and inorganic colloids. Therefore, by referring to the dissolved REEs as the fraction derived from 0.22 μm , we include colloidal particles. All the filtrates were stored in HDPE bottles that had been pre-washed with nitric acid and deionized water, and preserved with ultra-pure HNO_3 before being sent to the Géosciences Environnement Toulouse (GET) laboratories in Toulouse, France. Here, they were stored at 4 °C until processing. Because REEs are correlated with turbidity in certain South American rivers (de Campos and Enzweiler, 2016), we wished to test if the total suspended sediments (TSS) are correlated with the REEs. Therefore, the TSS were measured by filtering 500 mL of the water sample on a pre-weighed 0.45 μm pore-size cellulose acetate filter, and then measuring the difference in pre- and post-filtering filter weight. Data for monthly pH values were obtained from the Orinoco at Puerto Ordaz (8°16'25"N, 62°54'46"W, ~80 km downstream of Ciudad Bolívar). Here, systematic sampling campaigns were also carried out on a monthly basis between February 2003 and December 2008 (Mora et al., 2009, 2014, 2017). We considered these pH data because we did not detect significant pH variations between the two gauging stations during the hydrological year. This probably relates to the absence of large tributaries joining the Orinoco between Ciudad Bolívar and Puerto Ordaz. The 80 km distance between these two stations only represents 3.7% of the total 2140 km channel length of the Orinoco River from its headwater to the Orinoco estuary. Certain pH data (of 15 months from June 2007 to August 2008) have already been published (Mora et al., 2017) for the river sector OR5 at Puerto Ordaz. Similarly, dissolved organic carbon (DOC) data from the same period and river sector (Mora et al., 2014, 2017) were used in this study to establish correlations between the DOC with the remaining variables

presented here, during the same sampling periods.

The sampling campaigns in Ciudad Bolívar were carried out within the observatory system on the hydrology, sedimentology, and geochemistry of the Amazon, Congo, and Orinoco basins (SO-HyBam) program (www.so-hybam.org). The daily water discharges of the Orinoco River at Ciudad Bolívar were also provided by the SO-HyBam program.

3.2. Analysis of Fe, Al, and REEs

The concentrations of Al and Fe in the Orinoco water samples were measured at the GET laboratory by inductively coupled plasma-optical emission spectrometry (ICP-OES) on an IRIS Intrepid II XSP spectrometer (Thermo Electron Corp.). The REE concentrations were measured by inductively coupled plasma-mass spectrometry (ICP-MS) with AGILENT 7500 CE equipment using a four-point calibration curve and internal standards of In and Re to correct for instrumental drift and matrix effects. The correction for oxide and hydroxide ion-isobaric interferences was performed by measuring the oxide and hydroxide production ratio for each element and its isotopes using mono-elemental standard solutions (Aries et al., 2000). Overall, the contribution of the oxides ranged from 0.1 to 2.5% of the element ^{-16}M (depending on the element). Meanwhile, the contribution of the hydroxides was generally <0.1% of the element ^{-17}M . In fact, there were no relationships between the Ba concentrations and Gd and Eu anomalies. This indicates an adequate oxide and hydroxide interference correction (Gd anomalies were calculated as $\text{Gd}_{\text{UCC}} / (0.33\text{Sm}_{\text{UCC}} + 0.67\text{Tb}_{\text{UCC}})$). All the glassware used for the Al, Fe, and REE analysis was cleaned by washing with nitric acid and deionized water prior to use. The international reference material SLRS-5 (river water reference material for trace metals, certified by the National Research Council of Canada) was used to assess the accuracy and reproducibility of the REE measurements. Although the REE concentrations are not certified in the SLRS-5, the results (mean of three measurements) of the REE analysis in this reference material were in agreement (~16% for Gd, ~15% for Eu, and better than 10% for the other REEs) with the compiled values by Yeghicheyan et al. (2013). The results of the quality control analysis (measured and referenced SLRS-5 values) are presented in the Supplementary Material (Table S1) together with their respective standard deviations and the detection limit (DL) reported for REE analysis.

Because the Tm and Lu concentrations were below the DL of the analytical technique for five months (for Tm) and two months (for Lu) in 2007, the results of these values were expressed as DL/2 to perform statistical analysis and annual flux calculations. The Orinoco water discharge values used for statistical analysis were the respective water discharges presented by the Orinoco River on each sampling day. The non-parametric Spearman's correlation analysis was performed to identify correlations between the analyzed elements and the chemical parameters. The minimum significance for each statistical analysis was set at $p < 0.05$.

4. Results

Table 2S (Supplementary Material) presents the monthly concentration data for dissolved Fe, Al, and REEs measured in the Orinoco River at Ciudad Bolívar during 2007 and 2008, and the data for pH and DOC measured at Puerto Ordaz as reported by Mora et al. (2017). Because the REE data obtained during February, March, and April 2007 were very close to the reported DL, the uncertainties associated with these measurements may result in values higher than those expected. Therefore, the quantitative REE values reported here during these months should be considered with caution. Table 1 presents the ranges of pH and concentrations of dissolved Fe, Al, and individual REEs measured in the lower Orinoco River during both years. It also compares these data with previous studies of dissolved REE concentrations reported in other large rivers. The main feature of these results is the high

Table 1

Range of pH and dissolved Fe, Al, and REE concentrations in the Orinoco River and comparison with previous studies (Deberdt et al., 2002) and the range of dissolved REE concentrations in other large rivers. Temporal data of the Amazon, Madeira, Negro and Solimões rivers are from Barroux et al. (2006). Mississippi River data are from Shiller (2002). Data of the Xijiang (Xu and Han, 2009) and Yamuna (Rengarajan and Sarin, 2004) rivers do not correspond to seasonal variations. NR indicates non-reported values.

Element	Orinoco (this study)	Orinoco (previous)	Amazon River	Madeira River	Negro River	Solimões River	Mississippi River	Xijiang River	Yamuna River
pH	5.53–7.57	6.51	6.3–7.0	5.8–7.2	5.32–6.29	6.1–7.1	Around 7.8	7.56–8.63	7.1–9.1
Al (µg/L)	15.85–342.7	61.77	NR	NR	NR	NR	NR	NR	NR
Fe (µg/L)	5.94–988	142.4	NR	NR	NR	NR	NR	NR	NR
La (ng/L)	4.82–464	177.2	35–130	7–136	103–385	20–52	3.47–15.7	7.5–46.5	15–267
Ce (ng/L)	10.86–1276	520.7	69–325	13–311	323–1058	40–100	3.22–22	9.2–101.9	13.8–558
Pr (ng/L)	1.08–150	62.0	10–41	2–55	35–103	7–16	1.27–5.35	1.76–12.5	2.3–64.9
Nd (ng/L)	6.03–653	288.9	47–178	7–271	134–422	31–74	6.78–26.1	6.52–52.6	18.3–253
Sm (ng/L)	1.30–157	68.2	14–49	1–80	25–81	8–21	1.95–6.32	1.31–10.3	4.1–60.6
Eu (ng/L)	1.00–36.1	14.0	NR	NR	NR	NR	0.47–1.47	0.38–2.53	2.0–11.9
Gd (ng/L)	2.22–184.4	73.7	13–46	2–86	20–58	9–20	3.15–9.59	1.5–11.04	4.7–61
Tb (ng/L)	0.41–24.48	9.84	NR	NR	NR	NR	0.56–1.46	0.24–1.38	0.69–8.6
Dy (ng/L)	3.57–133.2	56.1	11–39	1–61	18–53	7–17	4.39–9.75	1.45–7.77	3.0–50.5
Ho (ng/L)	0.69–24.49	10.7	NR	NR	NR	NR	1.18–2.36	0.34–1.74	0.5–9.2
Er (ng/L)	1.81–65.35	31.5	7–22	1–29	11–32	4–11	3.8–7.5	1.03–5.21	1.3–27.9
Tm (ng/L)	<1.0–8.76	4.3	NR	NR	NR	NR	0.49–1.01	0.13–0.68	0.30–4.2
Yb (ng/L)	1.55–51.43	28.5	4–19	1–20	11–31	3–10	2.9–6.2	0.8–4.27	1.4–21.3
Lu (ng/L)	<0.60–7.57	4.27	NR	NR	NR	NR	0.47–0.98	0.13–0.64	0.5–3.0

abundance of REEs (maximum concentrations) in the Orinoco River in comparison to the other large rivers such as the Mississippi, Xijiang, Yamuna, and the Amazon and its main tributaries. This is also consistent with a study of the REE distribution in the Caribbean Sea, which observed high concentrations of REEs in the mouth of the Orinoco (Osborne et al., 2015). This study attributed the fluvial input of the Orinoco, rather than the Saharan dust supply, as the main REE source of the Caribbean seawater. Table 1 also indicates that previous Orinoco REE data reported by Deberdt et al. (2002) for the same sampling station (Ciudad Bolívar) fall within the range of the data reported here.

Similar to that in other large rivers worldwide, such as the Mississippi River and the Amazon River tributaries (Shiller, 2002; Barroux et al., 2006), the dissolved REE abundance in the Orinoco River varied seasonally by more than an order of magnitude (Table 1). Furthermore, with the exception of Eu, the concentrations of LREEs (La, Ce, Pr, Nd, and Sm) displayed a seasonal variation of up to two orders of magnitude. The HREEs displayed significantly lower seasonal variabilities, with the maximum variation being for Gd (up to 83-fold variation) and Tb (60-fold variation). Other HREE variations over the study period ranged from 9- to 37-fold.

Overall, a lower abundance of REEs was commonly observed during the low-water periods (i.e., March and April), whereas the maximum concentrations were frequently observed during periods of high-water discharge (i.e., August and September). This seasonal pattern of dissolved REEs observed in the Orinoco has also been reported for dissolved REEs in the Amazon River tributaries (Barroux et al., 2006), for Al and Fe concentrations in the lower Orinoco River (this study), and for other dissolved trace elements (Mn, Zn, Cu, and Cr) in different sections of the middle and lower Orinoco River (Mora et al., 2017). Each REE displayed highly significant positive correlations with the other REEs and with Al and Fe ($N = 24$, $p < 0.001$). Furthermore, all the REEs displayed significant negative correlations with pH ($N = 23$, $p < 0.05$, for Eu, Tm, and Lu; and $N = 23$, $p < 0.01$, for the remaining REEs). However, none of these were correlated with TSS. Fig. 2a shows the higher seasonal variation of LREEs compared to that of HREEs in the Orinoco River during the study period. Fig. 2b and c depict the seasonal variations of Al and Fe concentrations and the variability of pH and TSS in the lower Orinoco River during the study period, respectively.

5. Discussion

5.1. Factors controlling the content and fractionation of dissolved REEs

5.1.1. REE abundance in host rocks and suspended material

It is well established that REEs are a group of relatively insoluble elements that display little fractionation during erosional processes, and exhibit a similar signature as weathered rocks in most cases. In rivers, the REE abundance in both the dissolved and particulate phases is linked to the composition of host rocks and/or accessory minerals. With regard to the particulate phase, recent studies have demonstrated that REEs are more abundant in the suspended material of rivers that drain igneous and metamorphic terranes in comparison to rivers that drain volcanic rocks or sedimentary formations (Bayon et al., 2015). However, these studies also verify that the REE abundance and fractionation in the suspended material is also linked with the degree of alteration of sediments and the particular erosion regime in the basin (Bayon et al., 2015; Rousseau et al., 2019). Meanwhile, the abundance and fractionation of REEs in the dissolved phase depend on the composition of the weathered rocks and certain physicochemical properties of the river water, as well as on other important factors such as the presence of colloidal carrier phases, redox conditions in the source, and mixing between tributaries (Deberdt et al., 2002; Shiller, 2010).

The Orinoco River ranks third in terms of water discharge to the oceans. It also exhibits the highest seasonal variability of dissolved REE concentrations among the large rivers worldwide (Table 1). This large variation is caused by the high content of REEs in the weathered rocks and is driven by different geochemical processes that occur in the basin waters over the hydrological year. First, it is important to highlight the high abundance of REEs in the river's suspended material and in the host rocks of the Orinoco basin. The diverse lithological composition of the Andes hinders the establishment of a particular lithology as the point source of the REE content in the Orinoco waters. Nevertheless, 95% of the suspended material transported by the Orinoco River originates from these orogenic mountains. This material carries important information on the host rock's REE signature. In a recent study performed on the suspended material in large South American rivers, Rousseau et al. (2019) highlighted the relatively high concentrations of REEs in the suspended material of the Orinoco River. These REE concentrations were higher than those measured in the Amazon River sediments notwithstanding a higher chemical alteration in the Orinoco sediments. Meanwhile, although the Guayana Shield rivers account for only 5% of

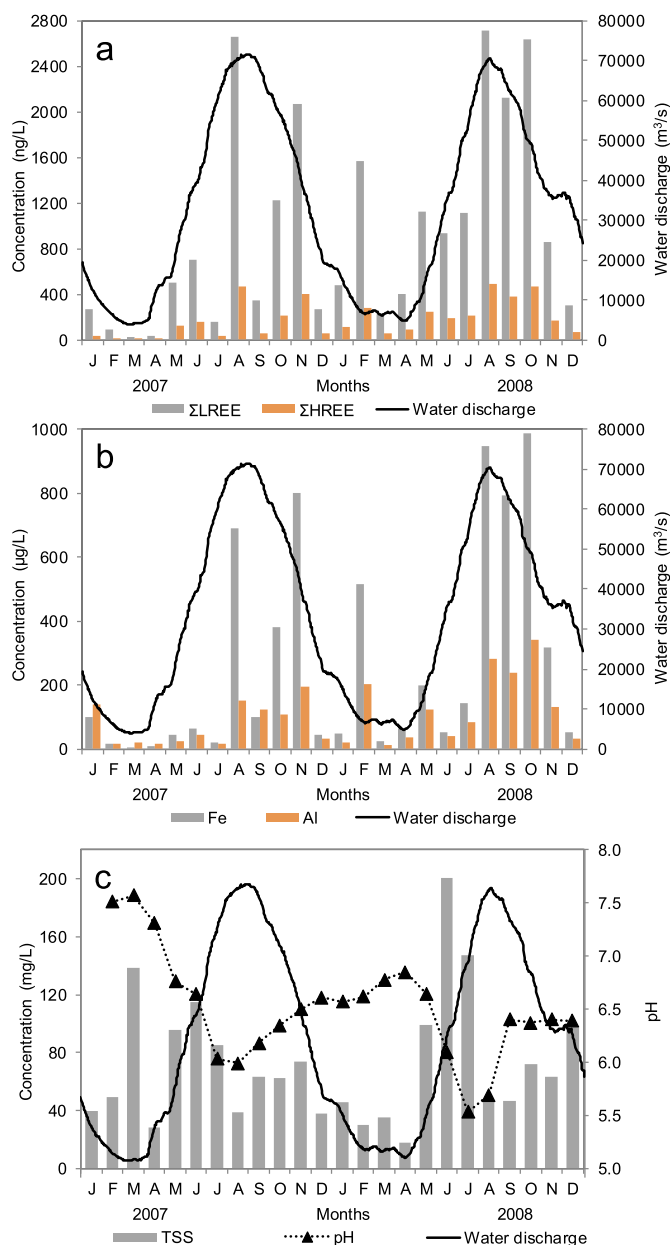


Fig. 2. Monthly patterns of dissolved LREE and HREE concentrations (a) and dissolved Al and Fe concentrations (b) together with the daily water discharge of the Orinoco River at Ciudad Bolívar. Seasonal patterns of TSS concentrations (measured in Ciudad Bolívar) and pH (measured in Puerto Ordaz; Mora et al., 2017) in the lower Orinoco River (c).

the Orinoco sediment load (Meade et al., 1990), the rivers draining this shield lithology have displayed the highest levels of dissolved REEs in the Amazon basin (Barroux et al., 2006). This is probably owing to the high content of REEs in the volcanic and granitic rocks of the southern shield area (Minuzzi et al., 2008; Rosa et al., 2014), which are released to rivers during weathering and stabilized by the low-pH and colloidal-rich water of the shield areas. This fact is discussed below.

5.1.2. pH and water discharge

One of the most prominent factors controlling the content of REEs in water is the pH-related adsorption/desorption process (Sholkovitz, 1992; Xu and Han, 2009). The Orinoco River has the intrinsic feature of showing high variations in pH and water discharge along the year (Mora et al., 2017), leading strong seasonal variations of dissolved REE concentrations. During the dry season, the minimum water discharge is

~4000 m³ s⁻¹, whereas a maximum discharge of 70 000 m³ s⁻¹ occurs during the rainy season. Thus, the maximum/minimum water discharge (Q_{\max}/Q_{\min}) ratio in the Orinoco ranges from 16 to 18. This is higher than that of the Mississippi River (10), middle Yangtze River (7.5), and Amazon River (2.4) and its major tributaries (Solimões, 2.9, Madeira, 11.4, and Negro, 4.8) (Espinoza Villar et al., 2009; Sivapragasam et al., 2014; Cheng et al., 2018). This high Q_{\max}/Q_{\min} ratio produces a high variability in the pH of the river water because the pH is controlled by the concentration of the bicarbonate (HCO_3^-) derived from silicate and carbonate rock weathering, which is in turn largely dependent on the dilution that relates to the Orinoco water discharge (Mora et al., 2017). In this context, the high variability of the Orinoco River discharge over a hydrological year induces considerable variations in the pH of the river water (Fig. 2c), thereby producing seasonal variations in the REE concentrations owing to the pH-related desorption process. In fact, the lowest REE concentrations are observed during periods of low water discharge (basic to circum-neutral pH), whereas the highest REE concentrations are observed during periods of high discharge (acidic conditions). It is also noteworthy that Madeira River is the Amazon tributary that displays the highest Q_{\max}/Q_{\min} ratio (11.4) and the highest variations in dissolved REE concentrations over the year (Barroux et al., 2006). This is consistent with the high Q_{\max}/Q_{\min} ratios and the strong seasonal variations of REEs displayed by the Orinoco River (Table 1).

Fig. 3 depicts the upper continental crust (UCC)-normalized dissolved REE concentration patterns (Taylor and McLennan, 1985) under the different pH conditions that were determined for selected months in the Orinoco River. This figure also compares these patterns with those of the Mississippi River (Shiller, 2002), Xijiang River (Xu and Han, 2009), and major tributaries of the Amazon River (Solimões, Madeira, and Negro) (Barroux et al., 2006). At first glance, the normalized REE patterns display a zig-zag distribution between neighbors during the low-water period (March and April). This zig-zag behavior is probably related to the high uncertainties associated with the REE measurements during these months, which were commented on above. Fig. 3 also shows that the UCC-normalized patterns vary during the hydrological year, demonstrating that REE fractionation can be altered seasonally. This figure depicts a marginal, albeit observable pH dependence of both the concentration and degree of fractionation of dissolved REEs in the Orinoco and the other large rivers. However, as we will discuss below, organic and inorganic colloids can also play an important role in both the abundance and fractionation degree of REEs in the river.

In general, the UCC-normalized patterns presented in Fig. 3 show a higher enrichment of HREEs in comparison with LREEs (except for Eu) at pH > 7. Nevertheless, as the pH decreases, the UCC-normalized REEs exhibit convex patterns that evidently indicate a decrease in the middle and heavy REE enrichments with regard to LREEs, which is also a typical behavior of dissolved REEs in large Amazonian rivers (Barroux et al., 2006). This behavior also agrees with those revealed by other studies performed in rivers that report a preferential release from the particulate phase to the dissolved pool of LREEs over that of the HREEs at lower pH values (Sholkovitz, 1995). During the high discharge period (August and September), the convex pattern becomes more pronounced (Fig. 3) although the pH is not as acidic. This behavior appears to be related to the effect of Al- and Fe-colloids in the REE fractionation and will be discussed in the following section. Notwithstanding the convex patterns displayed by REEs, the $\text{Gd}_{\text{UCC}}/\text{Nd}_{\text{UCC}}$ ratios (not shown), which are measures of middle/light REE fractionation, did not exhibit any trend with the pH, water discharge, or Fe and Al concentrations.

Fig. 4 shows the pH values in the Orinoco waters versus the UCC-normalized Yb/Nd ratios ($\text{Yb}_{\text{UCC}}/\text{Nd}_{\text{UCC}}$), which have been observed to provide a measure of the HREE/LREE fractionation in river water. The $\text{Yb}_{\text{UCC}}/\text{Nd}_{\text{UCC}}$ ratios range from 0.88 to 1.65 at pH < 7, with no significant trends at acidic pH. Conversely, as depicted in Fig. 3, there is an increase in the $\text{Yb}_{\text{UCC}}/\text{Nd}_{\text{UCC}}$ ratios at pH > 7 (ratios of up to 4.5). This indicates a more fractionated composition of dissolved REEs relative to

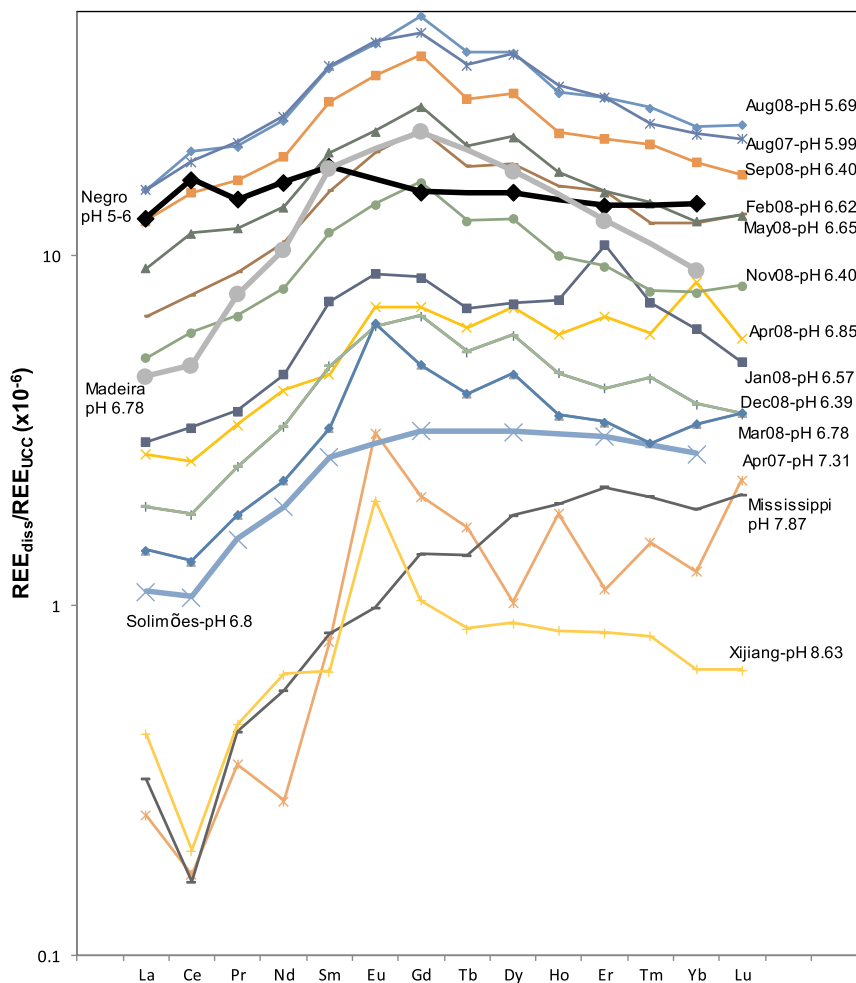


Fig. 3. UCC-normalized REE patterns in the dissolved load under different pH conditions in the lower Orinoco River and comparison with the same patterns reported for the Mississippi, Xijiang, Solimões, Madeira and Negro rivers.

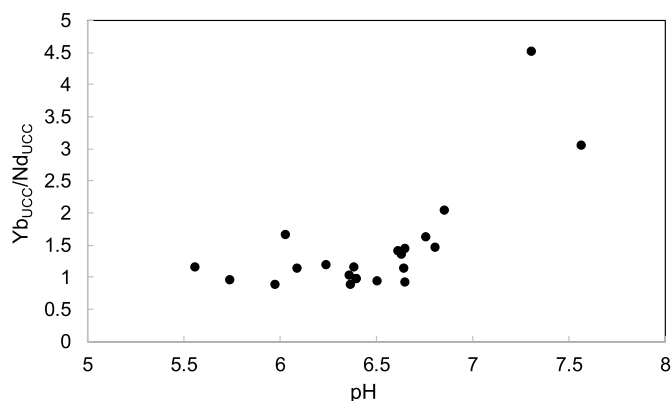


Fig. 4. Scatter diagram showing the UCC-normalized Yb/Nd ratios versus pH in the Orinoco River.

the crustal abundance for slightly alkaline water. The enrichment in HREEs relative to LREEs in circumneutral and alkaline water has been reported for the Amazon and Solimões rivers (Barroux et al., 2006) and for the Mississippi River (Shiller, 2002). The latter exhibited dissolved Yb_{UCC}/Nd_{UCC} ratios ranging from 2.1 to 8.1 at $pH \sim 7.8$. Conversely, the more acidic waters of the Negro River (pH between five and six) presented Yb_{UCC}/Nd_{UCC} ratios < 1 , with no significant trends between the ratios and pH or hydrological variations (Barroux et al., 2006). Indeed,

this agrees with our observations in the Orinoco River.

5.1.3. Role of organic and inorganic colloids in the transport and fractionation of REEs

The other important factor that accounts for the high REE concentrations (and thereby, the broad REE concentration range) is the input of REEs from tributaries flowing from the Guayana Shield and the input from the floodplain. As commented above, the volcanic and granitic rocks and several alluvial deposits of the southern Guayana Shield are rich in REEs (Minuzzi et al., 2008; Rosa et al., 2014). In this transport-limited environment, where low physical erosion rates result in the development of thick soil horizons, intense rainfall events promote the mobilization of organic and inorganic colloids from surface and intermediate soil layers to rivers. These colloids are considered the most significant REE-carrier phases, given that REEs can be bound to organic colloids to form organic complexes (Dupré et al., 1999; Benedetti et al., 2002; Stolpe et al., 2013; Matsunaga et al., 2015) and can be scavenged by mineral colloids of Fe and Al (Fe- and Al-oxyhydroxides), thereby affecting their fractionation during transport (Pokrovsky et al., 2006; Luo et al., 2016). Similarly, the water draining the Guayana Shield areas is predominantly acidic, which aids in stabilizing the REEs in solution. In this context, given that high rainfall (between 3000 and 4500 mm) is frequently observed in the southern Guayana Shield during the wet season (Machado-Allison et al., 2003; Flores et al., 2008), there is an important input of dissolved REE-rich water from the Guayana Shield to the Orinoco mainstream (50% of the Orinoco water flows from the Guayana Shield). This may contribute to increasing the dissolved

REE pool in the Orinoco during high-water periods.

In addition to the Guayana Shield input, the floodplain of the Orinoco River can also considerably contribute to the pool of dissolved REEs in the Orinoco during flood periods. The lower part of the Orinoco River has a fringed floodplain of approximately 7000 km². It includes 2294 permanent floodplain lakes (Hamilton and Lewis, 1990) that are connected to the river for four–six months of the year during the high discharge period. In this extensive floodplain, which is considered as a weathering reactor (Bouchez et al., 2012), the DOC is produced by the decomposing litter of the flooded vegetation (Hedges et al., 1994). Similarly, the flooded wetlands function as a source of redox-sensitive elements (e.g., Fe and Mn) owing to the reducing conditions (Viers et al., 2005). Both DOC and redox-sensitive elements (in conjunction with Al-colloids) are constituted by organic- and inorganic-colloids, respectively, which can transport considerable amounts of dissolved REEs from the floodplain to the Orinoco mainstream. A similar phenomenon in the Amazon basin has been indicated by Barroux et al. (2006), where the concentrations of individual dissolved REEs in the floodplain water exceed those of the Amazon River mainstream during flood periods.

Although organic colloids exhibit the capacity to complex REEs, DOC was not observed to correlate with any REE (N = 15) in the Orinoco River. Meanwhile, Fig. 5a and b reveal statistically significant correlations ($p < 0.001$) between the sum of the dissolved LREE and HREE concentrations (Σ LREE and Σ HREE) versus the concentrations of dissolved Al and Fe. These correlations indicate the scavenging of both LREEs and HREEs by Al- and Fe-colloids. From this perspective, it is valid to affirm that mineral Fe- and Al-colloids play a determining role in the REE abundance for the $<0.22 \mu\text{m}$ fraction, and that the organic

complexation of REEs is overshadowed by Al- and Fe-mineral scavenging in the Orinoco River. Fig. 5a and b also show that the slope of the linear regression is more prominent for LREEs than for HREEs. This is likely to be owing to the higher scavenging capacity of LREEs relative to HREEs on mineral colloidal particles (Sholkovitz, 1995; Matsunaga et al., 2015). Because both the Al and Fe concentrations in the Orinoco River are low under circumneutral-pH conditions, it is valid to assume that the relationships of Al and Fe with REEs in terms of their concentration are correlative although not causative (fortuitous correlation between Fe, Al, and REEs). Nevertheless, Fig. 3 indicates that REE concentrations do not exhibit a strict relationship with pH (i.e., although the pH is lower in December, there are lower REE concentrations during December 2008 than during February and May 2008). This indicates the involvement of other processes (complexation and scavenging) in the abundance of REEs in the river. Furthermore, ultrafiltration studies performed by Deberdt et al. (2002) in large South American and African rivers (including the Orinoco) demonstrated that the mineral colloidal fraction may account for over 60% of the total REE content present in the solution phase ($<0.20 \mu\text{m}$) irrespective of the pH (moderately acidic to basic).

With regard to the role of colloids in the REE fractionation, Fig. 3 depicts that the UCC-normalized REEs display more pronounced convex patterns during flood/high-water periods. This middle REE enrichment has been observed in several river waters and has been attributed to the weathering of middle REE-enriched oxy-hydroxides of Fe and Mn and the presence of middle REE-enriched organic and/or inorganic colloids (Elderfield et al., 1990; Sholkovitz, 1995; Johannesson and Zhou, 1999; Ingri et al., 2000; Johannesson et al., 2004; Shiller, 2010). However, as commented earlier, the Gd_{UCC}/Nd_{UCC} ratios (which measure the

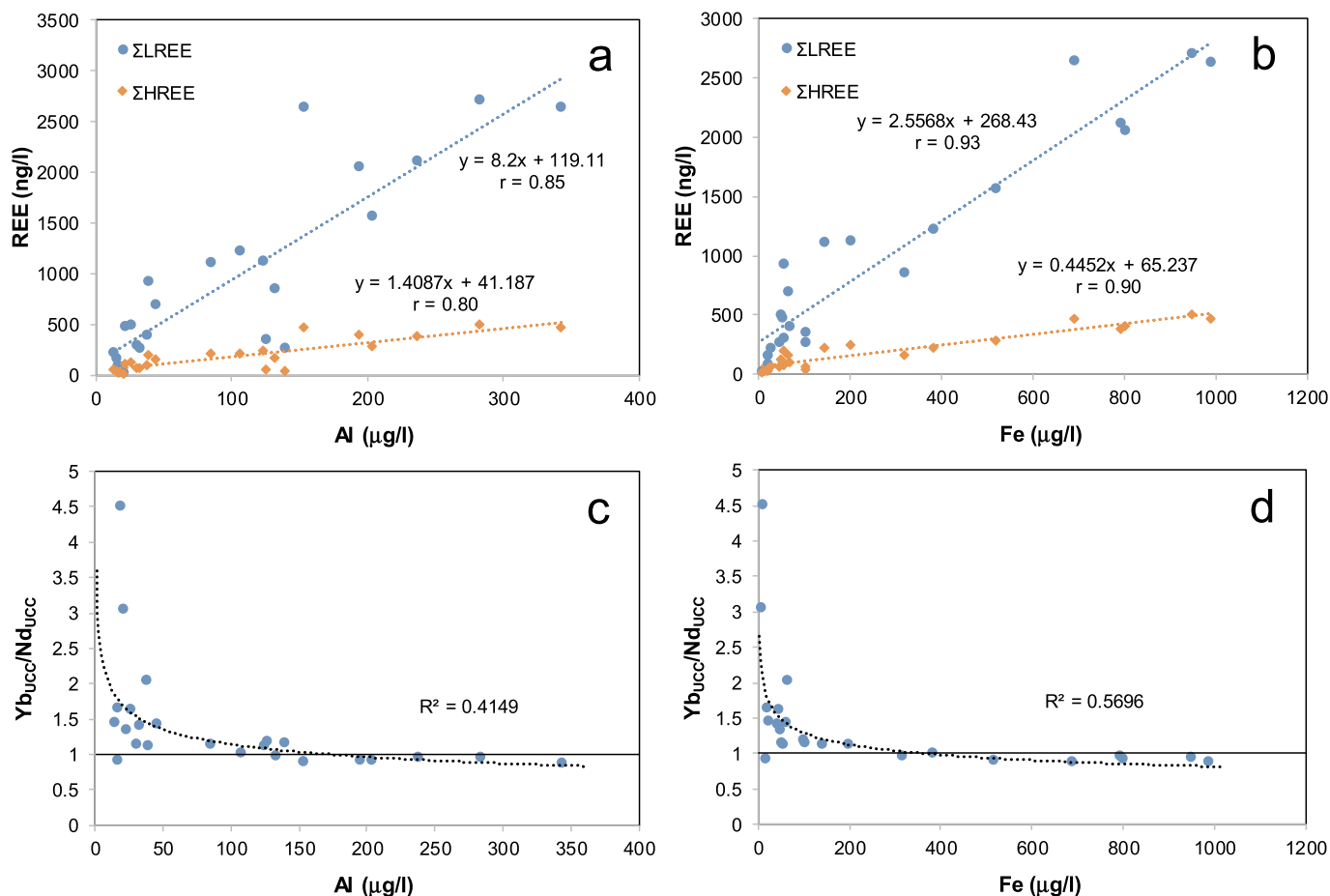


Fig. 5. Relationships between Σ LREEs and Σ HREEs versus Al (a) and Fe (b) concentrations in the Orinoco River. Scatter diagrams of the UCC-normalized Yb/Nd ratios versus the concentrations of Al (c) and Fe (d) in the Orinoco River.

middle/light REE fractionation) did not display correlation with Al, Fe, or DOC concentrations. Meanwhile, the progressive enrichment of LREEs relative to HREEs appears to be driven by the abundance of inorganic Fe- and Al-colloids in river water. Fig. 5c and d depict the inverse relationships between the Yb_{UCC}/Nd_{UCC} ratios and the Al and Fe concentrations, which fit a logarithmic model. This indicates that the Yb_{UCC}/Nd_{UCC} ratios decline rapidly as the Al and Fe concentrations increase. That is, Al- and Fe-mineral colloids increase the dissolved REE abundance and also produce a progressive enrichment of LREEs relative to HREEs. This progressive enrichment of LREEs relative to HREEs tends to an asymptotic value of $Yb_{UCC}/Nd_{UCC} = 1$, which implies negligible or no fractionation.

5.2. Ce and Eu anomalies

Unlike the other REEs that are present in the oxidation state of +3, Ce and Eu can also exist in the +4 and +2 states, respectively. This property enables both the elements to display different chemical behaviors and degrees of fractionation with respect to their neighbors, thereby resulting in Ce and Eu anomalies. The Ce-anomaly [$Ce\text{-anomaly} = 3Ce_{UCC}/(2La_{UCC} + Nd_{UCC})$] and Eu-anomaly [$Eu\text{-anomaly} = 2Eu_{UCC}/(Sm_{UCC} + Gd_{UCC})$] were calculated using the UCC-normalized concentrations of their neighbors, as reported elsewhere (Sholkovitz, 1995; Smith and Liu, 2018).

The Ce-anomaly ranged between 0.65 and 1.14 and displayed a strong dependence on hydrological variations, specifically with regard to the water discharge. Negative Ce-anomalies were commonly observed during low-water periods (February–April, Ce-anomaly range = 0.65–0.92), whereas no Ce-anomalies (Ce-anomaly range = 0.92–1.14) were observed during the remaining months (we note that interpolated ratios close to one were not considered as anomalies because of analytical uncertainties). This leads to a significant positive correlation between the Ce-anomaly and water discharge ($N = 24$, $r = 0.59$, $p < 0.01$). This hydrological control on Ce-anomalies could be explained by the variations in the lithological inputs over the hydrological year. During the low-water period, the Orinoco River receives important contributions from the Andes, where silicate and carbonate rocks dominate. Thus, the aqueous Ce-anomaly values in Orinoco River can exhibit a signature similar to that observed in certain Andean host rocks, which have Ce-anomaly values up to 0.53 (Conde-Gómez et al., 2018). This Ce-anomaly signal during low-water is in agreement with other works performed in alkaline rivers or waters draining carbonates. In these works as well, negative Ce-anomaly values have been observed in water in conjunction with a depletion of dissolved LREEs relative to HREEs (Johannesson et al., 2000; Rengarajan and Sarin, 2004; Xu and Han, 2009). Apart from the signature acquired from host rocks, this can occur because unlike the other trivalent lanthanides, Ce (III) (which is the dominant species at low pH) can be oxidized to Ce (IV) at a higher pH to form CeO_2 , which is in turn adsorbed by mineral surfaces (Goldstein and Jacobsen, 1988; Sholkovitz, 1992). Nevertheless, this process by itself does not appear to control the variability of dissolved Ce in the lower Orinoco River during the entire hydrological year, because the significant positive correlation between the Ce-anomalies and Ce concentrations ($N = 24$, $r = 0.48$, $p < 0.05$) indicates that adsorption of Ce (III) by mineral surfaces and Al- and/or Fe-colloidal scavenging can be the most important factors in controlling the dissolved Ce seasonality in the river.

With regard to the flood/high-water periods, the large contribution of the water flowing from the shield areas and flooded Orinoco savannas can modify the negative Ce-anomaly values observed during low-water periods. First, unlike Andean rocks, the igneous rocks and Paleoproterozoic granites of the Guayana Shield do not display negative Ce-anomalies (Schulze et al., 2006; Almeida et al., 2007). This agrees with the positive Ce-anomalies (between 1.2 and 1.3) displayed by the Negro River water over the entire hydrological year (Barroux et al., 2006). Meanwhile, the influence of the more reduced conditions in the

floodplain can also affect the Ce-anomaly signal in the lower Orinoco mainstream. In the over 7000 km² of flooded areas, biological reduction occurs during the decomposition of submerged vegetation, thus inducing a lesser Ce fractionation during weathering in this less oxidizing environment. This is consistent with the highest dissolved Fe and Mn concentrations observed in the Orinoco River during the high-water stage (Mora et al., 2017), which reveal that the Orinoco River water is more influenced by reducing sources during this stage. This Ce-anomaly behavior has also been observed in the Loch Vale Watershed (Colorado), where less oxidized/more reduced source conditions during spring resulted in lower Ce fractionated values in water (Shiller, 2010). Therefore, the contribution of both Guayana Shield water and sources where less oxidized/more reduced conditions dominate (floodplain water) during flood/high-water periods can alter the Ce-anomaly signal toward less fractionated values in the lower Orinoco River, as depicted in the UCC-normalized patterns for August and September in Fig. 3.

In contrast to the Ce-anomalies, the Eu-anomalies were positive and relatively higher during low-water periods (1.22–2.59), whereas Eu-anomaly values close to one were observed during the rest of the hydrological year. This variability promotes the occurrence of a significant negative correlation between Eu-anomalies and water discharge ($N = 24$, $r = -0.59$, $p < 0.01$). The increase in the Eu-anomalies during the low-water stage indicates the preferential dissolution of Eu-bearing minerals during this stage. As mentioned previously, 50% of the Orinoco River water flows from the Precambrian Guayana Shield, where plagioclases (albite and Ca-silicates) and K-feldspar minerals are abundant in the regional granites. The enrichment of Eu in plagioclases over the other REE-bearing primary minerals is well established. It occurs because Eu is preferentially incorporated into plagioclase in its reduced form, Eu (II) (Aubert et al., 2001), thereby replacing Ca in a reducing magma. Similarly, although the Andean orogenic mountains are composed of highly diverse lithologies, several works have reported positive Eu-anomalies in rock formations (Conde-Gómez et al., 2018). Therefore, preferential weathering of plagioclases and Eu-bearing minerals in both the Guayana Shield and Andes should result in positive aqueous Eu-anomaly during the entire hydrological year. Nonetheless, the input of water that has weathered sedimentary material with negative Eu-anomalies may decrease the Eu-anomaly signal in the river water during the flood periods. Although the composition of REEs in the sediments of the Orinoco River floodplain has not been assessed, we consider the fact that the floodplain sediments of large rivers display the common characteristic of highly negative Eu-anomalies (Roddaz et al., 2014; Pang et al., 2018). Thereby, positive Eu-anomalies in water can decrease during peak flow and flood periods owing to the intense weathering of floodplain sediments with negative Eu-anomalies (Stallard et al., 1991; Bouchez et al., 2012; Moquet et al., 2016). In contrast, aqueous Eu-anomalies can increase during dry periods when the river water does not enter the floodplain and the groundwater draining Guayana Shield and Andean lithologies is the main source of water to the Orinoco mainstream.

5.3. Annual dissolved REE fluxes from Orinoco River to Orinoco estuary

Table 2 presents the individual annual dissolved REE fluxes introduced by the Orinoco River to the Orinoco estuary during 2007 and 2008. These fluxes were calculated by first multiplying the monthly concentrations of individual REEs by the daily water discharge of the Orinoco River that were measured at the Ciudad Bolívar gauging station. The daily fluxes were then summed for each day of each year. It is important to mention that downstream of Ciudad Bolívar, there is another important blackwater tributary to the Orinoco River (Caroní River). It presents an average water discharge of $\sim 4800 \text{ m}^3 \text{ s}^{-1}$. Nevertheless, given the low dissolved REE concentrations reported for this river in comparison to those of the Orinoco (Deberdt et al., 2002) and the fact that the Caroní River discharge is strongly regulated by

Table 2

Individual dissolved REE fluxes from the Orinoco River to the Orinoco estuary during this study.

Element	Annual Flux 2007(Ton y ⁻¹)	Annual Flux 2008(Ton y ⁻¹)	Average(Ton y ⁻¹)
La	192.6	286.7	239.7
Ce	505.1	750.7	627.9
Pr	61.2	90.1	75.6
Nd	277.0	395.4	336.2
Sm	68.5	97.2	82.9
Eu	15.6	22.7	19.2
Gd	71.5	111.9	91.7
Tb	10.1	14.7	12.4
Dy	58.5	82.4	70.5
Ho	10.7	14.8	12.7
Er	29.2	40.8	35.0
Tm	3.7 ^a	5.4	4.5
Yb	23.8	33.1	28.5
Lu	3.5 ^a	4.7	4.1

^a The annual fluxes were calculated taking into account 5 (for Tm) and 2 (for Lu) monthly concentrations below the detection limit.

hydroelectric dams along its course, our estimate of the Orinoco's dissolved REE fluxes to the estuarine zone is not likely be strongly affected by the Caroni River input.

The two year average of the data collected during this study indicates that the annual individual REE fluxes in the Orinoco River at Ciudad Bolívar varied from 4.1 t for Lu to 627.7 t for Ce. In general, all the individual REE fluxes increased in 2008 with respect to 2007. In 2008, the lowest flux increase was for Lu (45.6%), and the maximum was for Gd (56.5%). This discrepancy between the years is mainly related to the significant inter-annual variations in the REE concentrations, because the average annual water discharge from the Orinoco River displayed minimal variations between 2007 (34 477 m³ s⁻¹) and 2008 (32 378 m³ s⁻¹). It is important to mention that the fluxes calculated during this study should not be considered as the "true" dissolved REE fluxes from the Orinoco to the Atlantic Ocean. This is because of the well-known salinity-induced coagulation of riverine colloids in estuaries, which induces a large REE removal from the dissolved phase (Sholkovitz, 1995). Conversely, other REEs are present mainly in the solid phase (suspended sediments), and they are released to the ocean by desorption and/or dissolution when salinity increases again, as is the case for Nd (Rousseau et al., 2015).

Among the REEs analyzed in this study, Nd is of broad interest to the oceanographic community because the seawater Nd isotopic ratio is used to trace past and modern oceanic circulation patterns (Tachikawa et al., 2017). However, oceanic circulation models have estimated a large additional "missing flux" of Nd to oceans. This "missing" Nd annual flux ranges from 8 to 11 t and has been attributed to the release of Nd from continental margins (Tachikawa, 2003; Arsouze et al., 2009). Moreover, although dissolved Nd exhibits a non-conservative behavior during river water-seawater interactions owing to the flocculation of colloids (~95% of riverine Nd is removed from solution), re-dissolution of Nd can occur at a higher salinity (Sholkovitz, 1993). Therefore, it is essential to estimate the present dissolved Nd fluxes from rivers to oceans and their inter-annual variations, through time series. The average annual Nd flux from the Orinoco to the Orinoco estuary during this study was 336 t, with an inter-annual variation of 42.7% between 2007 and 2008. Because the quantity of re-dissolved Nd in the high salinity regions of the Orinoco estuary has not been ascertained, we can only estimate the lowest and highest contributions of the Orinoco River to the oceans by assuming 0% and 100% Nd re-dissolution, respectively. If all the removed Nd (95% of the total dissolved Nd input) is not re-dissolved in the high salinity zone, the Orinoco River contributes approximately 0.4% of the total annual Nd flux to the Atlantic Ocean (4300 t), and ~0.2% of the total annual dissolved Nd flux to the global oceans (8600 t), when using the total fluxes reported by Tachikawa

(2003). However, if we assume that 100% of the dissolved Nd input from the Orinoco is re-dissolved subsequently from flocculated colloids in the Orinoco estuarine zone, the Orinoco River contributes 7.8% and 3.2% of the total annual Nd flux to the Atlantic Ocean and global oceans, respectively. Our maximum annual Nd flux estimate is lower than that calculated by Barroux et al. (2006) for the Amazon River (607 t) using identical pore size filters (0.22 μm). Although the dissolved Nd flux of the Amazon River is almost two times that of the Orinoco River, the average annual water discharge of the Orinoco is six-times lower than the 209 000 m³ s⁻¹ discharged annually by the Amazon River to the Atlantic Ocean. Hence, the results presented in this paper highlight the important input of dissolved Nd and other REEs from the Orinoco River to the oceans, a fact that has been previously reported for the Caribbean Sea (Osborne et al., 2015). Finally, owing to the recent discovery of the rapid Nd release from lithogenic sediments in the Amazon estuary (Rousseau et al., 2015), there is an urgent need to quantify the Nd flux from the suspended sediments in the Orinoco estuary to improve our understanding of the dissolved Nd budget in the global oceans.

6. Conclusions

The Orinoco River exhibits the broadest range of dissolved REE concentrations when compared with other large rivers worldwide. This broad range is produced by hydrologically driven processes such as the seasonal variations in the input of organic and inorganic colloidal REE-carrier phases (e.g., DOC, and Al- and Fe-oxyhydroxides) and the seasonal variations in pH and water discharge. The waters flowing from the Guayana Shield and from flooded areas during flood/high-water periods dilute the carbonate concentrations and transport organic/inorganic colloids to the Orinoco mainstream. This decreases the pH and increases the abundance of REE-carrier phases (organic and inorganic colloids) during this period. Overall, these hydrologically driven variations result in a broad REE concentration range over the hydrological year in the Orinoco.

Fe- and Al-colloids appear to play a determining role in the dissolved REE abundance and overshadows the role of organic complexation. The fractionation of REEs is also dependent on the pH and the abundance of Al- and Fe-colloids. Alkaline pH values and low abundance of Al and Fe in the dissolved fraction result in a higher level of fractionation, wherein HREEs are strongly enriched with respect to LREEs. Meanwhile, more acidic water and the high abundance of Al- and Fe-inorganic colloids produce convex UCC-normalized REE patterns, indicating a significant reduction in the HREE enrichment with respect to that of LREEs. This behavior indicates that LREEs are more susceptible to adsorption by particulate material than HREEs, at circumneutral or alkaline pH values. Similarly, the enrichment of the dissolved LREE abundance relative to the continental crust at an acidic pH is also related to the increased binding capacity of LREEs to organic and inorganic Al- and Fe-colloids, which are abundant in the Orinoco River during low-pH periods (high-water periods).

The highest Ce fractionation and therefore, more negative Ce-anomalies occur during low water discharge periods because this Ce signal is acquired from Andean host rocks. However, a lesser Ce fractionation in more reduced environments (e.g., floodplains) can vary the Ce-anomaly signal to less fractionated values in the Orinoco mainstream during flood/high-water periods. The substantial input of water that has drained plagioclases and Eu-bearing minerals results in positive Eu anomalies in the dissolved phase during the low-water stage. However, a lower Eu fractionation with respect to its nearest neighbors is observed during flood periods. This is probably owing to the weathering of sedimentary material with negative Eu anomalies.

Notwithstanding the lower water discharge by the Orinoco River than that by the Amazon River, the former can contribute significant inputs of dissolved Nd and other dissolved REEs to the Atlantic Ocean and Caribbean Sea. The calculated annual fluxes to the Orinoco estuary displayed variations of up to 56% between the two studied years. This

fact reveals the importance of performing inter-annual REE time series in large rivers to better quantify the REE fluxes from rivers to the oceans.

Declaration of interests

The authors declare that they have no known competing financial interests or personal relationships that could have appeared to influence the work reported in this paper.

Acknowledgments

The authors wish to thank all the French and Venezuelan participants involved in the SO-HyBam (www.so-hybam.org) and ECOS/NORD/V07U02 (2007–2011) projects, and their institutions (IMF-UCV and CIEG-UNEG for Venezuela, and GET and IRD for France) for their contributions and support during this study. The constructive comments of two anonymous reviewers are also acknowledged. This work was supported by the SO-HyBam project and Université Paris 13 (project ECOS/NORD/V07U02), France.

Appendix A. Supplementary data

Supplementary data to this article can be found online at <https://doi.org/10.1016/j.apgeochem.2019.104462>.

References

- Almeida, M.E., Macambira, M.J.B., Oliveira, E.C., 2007. Geochemistry and zircon geochronology of the I-type high-K cal-alkaline and S-type granitoid rocks from southeastern Roraima, Brazil: Orosirian collisional magmatism evidence (1.97–1.96 Ga) in central portion of Guyana Shield. *Precambrian Res* 155, 69–97. <https://doi.org/10.1016/j.precamres.2007.01.004>.
- Aries, S., Valladon, M., Polvé, M., Dupré, B., 2000. A routine method for oxide and hydroxide interference corrections in ICP-MS chemical analysis of environmental and geological samples. *Geostand. Newsl.* 24, 19–31. <https://doi.org/10.1111/j.1751-908X.2000.tb00583.x>.
- Arsouze, T., Dutay, J.C., Lacan, F., Jeandel, C., 2009. Reconstructing the Nd oceanic cycle using a coupled dynamical-biogeochemical model. *Biogeosciences* 6, 2829–2846. <https://doi.org/10.5194/bg-6-2829-2009>.
- Aubert, D., Stille, P., Probst, A., 2001. REE fractionation during granite weathering and removal by waters and suspended loads: Sr and Nd isotopic evidence. *Geochem. Cosmochim. Acta* 65, 387–406. [https://doi.org/10.1016/S0016-7037\(00\)00546-9](https://doi.org/10.1016/S0016-7037(00)00546-9).
- Barroux, G., Sonke, J.E., Viers, J., Boaventura, G., Godderis, Y., Bonnet, M.P., Sondag, F., Gardoll, S., Lagane, C., Seyler, P., 2006. Seasonal dissolved rare earth element dynamics of the Amazon River main stem, its tributaries, and the Curuaí floodplain. *Geochem. Geophys. Geosyst.* 7, 1–18. <https://doi.org/10.1029/2006GC001244>.
- Bayon, G., Toucanne, S., Skonieczny, C., André, L., Bermell, S., Cheron, S., Dennielou, B., Etoubleau, J., Freslon, N., Gauchery, T., Germain, Y., Jorry, S.J., Ménot, G., Monin, L., Ponzevera, E., Rouget, M.L., Tachikawa, K., Barrat, J.A., 2015. Rare earth elements and neodymium isotopes in world river sediments revisited. *Geochem. Cosmochim. Acta* 170, 17–38. <https://doi.org/10.1016/j.gca.2015.08.001>.
- Benedetti, M., Ranville, J.F., Ponthieu, M., Pinheiro, J.P., 2002. Field-flow fractionation characterization and binding properties of particulate and colloidal organic matter from the Rio Amazon and Rio Negro. *Org. Geochem* 33, 269–279. [https://doi.org/10.1016/S0146-6380\(01\)00159-0](https://doi.org/10.1016/S0146-6380(01)00159-0).
- Berner, E., Berner, R., 1987. *The Global Water Cycle: Geochemistry and Environment*. Prentice-Hall, Inc, Englewood Cliffs, New Jersey, p. 397.
- Bouchez, J., Gaillardet, J., Lupker, M., Louvat, P., France-Lanord, C., Maurice, L., Armijos, E., Moquet, J.S., 2012. Floodplains of large rivers: weathering reactors or simple silos? *Chem. Geol.* 332–333, 166–184. <https://doi.org/10.1016/j.chemgeo.2012.09.032>.
- Cheng, L., Opperman, J.J., Tickner, D., Speed, R., Guo, Q., Chen, D., 2018. Managing the three Gorges dam to implement environmental flows in the Yangtze River. *Front. Environ. Sci.* 6, 64. <https://doi.org/10.3389/fenvs.2018.00064>.
- Cidu, R., Biddau, R., 2007. Transport of trace elements under different seasonal conditions: effects on the quality of river water in a Mediterranean area. *Appl. Geochem.* 22, 2777–2794. <https://doi.org/10.1016/j.apgeochem.2007.06.017>.
- Conde-Gómez, J., Naranjo-Vesga, J.-F., Mantilla-Figueroa, L.-C., 2018. Fluid inclusions and rare earth elements (REE) analysis in calcite veins: tectonic - Diagenesis interaction in the Rosablanca Formation, Mesa de Los Santos sector, Eastern Cordillera, Colombia. *C.T.F. Cienc. Tecnol. Futuro* 8, 31–43. <https://doi.org/10.29047/01225383.89>.
- de Campos, F., Enzweiler, J., 2016. Anthropogenic gadolinium anomalies and rare earth elements in the water of Atibaia River and Anhumas Creek, Southeast Brazil. *Environ. Monit. Assess.* 188, 281. <https://doi.org/10.1007/s10661-016-5282-7>.
- Deberdt, S., Viers, J., Dupré, B., 2002. New insights about the rare earth elements (REE) mobility in river waters. *B. Soc. Geol. Fr.* 173, 147–160.
- Dupré, B., Viers, J., Dandurand, J.L., Polve, M., Bénézeth, P., Vervier, P., Braun, J.J., 1999. Major and trace elements associated with colloids in organic-rich river waters: ultrafiltration of natural and spiked solutions. *Chem. Geol.* 160, 63–80. [https://doi.org/10.1016/S0009-2541\(99\)00660-1](https://doi.org/10.1016/S0009-2541(99)00660-1).
- Duvert, C., Condón, D.I., Raiber, M., Seidel, J.L., Cox, M.E., 2015. Seasonal and spatial variations in rare earth elements to identify inter-aquifer linkages and recharge processes in an Australian catchment. *Chem. Geol.* 396, 83–97. <https://doi.org/10.1016/j.chemgeo.2014.12.022>.
- Elderfield, H., Upstill-Goddard, R., Sholkovitz, E.R., 1990. The rare earth elements in rivers, estuaries, and coastal seas and their significance to the composition of ocean water. *Geochem. Cosmochim. Acta* 54, 971–991. [https://doi.org/10.1016/0016-7037\(90\)90432-K](https://doi.org/10.1016/0016-7037(90)90432-K).
- Espinoza Villar, J.C., Guyot, J.L., Ronchail, J., Cochonneau, G., Filizola, N., Fraizy, P., Labat, D., de Oliveira, E., Ordoñez, J.J., Vauchel, P., 2009. Contrasting regional discharge evolutions in the Amazon basin (1974–2004). *J. Hydrol.* 375, 297–311. <https://doi.org/10.1016/j.jhydrol.2009.03.004>.
- Flores, A.L., Briceno, H., Señaris, J.C., Velásquez, G., 2008. Descripción general de la cuenca alta del río Paragua, Estado Bolívar, Venezuela. In: Señaris, J.C., Lasso, C.A., Flores, A.L. (Eds.), *Evaluación Rápida de la Biodiversidad de los Ecosistemas Acuáticos de la Cuenca del Río Paragua, Estado Bolívar, Venezuela. RAP Bulletin of Biological Assessment* 49. Conservation International, Arlington, USA, pp. 47–53.
- Gaillardet, J., Dupré, B., Allègre, C.J., Nègre, P., 1997. Chemical and physical denudation in the Amazon River basin. *Chem. Geol.* 142, 141–173. [https://doi.org/10.1016/S0009-2541\(97\)00074-0](https://doi.org/10.1016/S0009-2541(97)00074-0).
- García, M.G., Lecomte, K.L., Pasquini, A.I., Formica, S.M., Depetris, P.J., 2007. Sources of dissolved REE in mountainous streams draining granitic rocks, Sierras Pampeanas (Córdoba, Argentina). *Geochem. Cosmochim. Acta* 71, 5355–5368. <https://doi.org/10.1016/j.gca.2007.09.017>.
- Gerard, M., Seyler, P., Benedetti, M.F., Alves, V.P., Boaventura, G.R., Sondag, F., 2003. Rare earth elements in the Amazon basin. *Hydrol. Process.* 17, 1379–1392. <https://doi.org/10.1002/hyp.1290>.
- Goldstein, S.J., Jacobsen, S.B., 1988. Rare earth elements in river waters. *Earth Planet. Sci. Lett.* 89, 35–47. [https://doi.org/10.1016/0012-821X\(88\)90031-3](https://doi.org/10.1016/0012-821X(88)90031-3).
- Haley, B.A., Du, J., Abbott, A.N., McManus, J., 2017. The impact of benthic processes on rare earth element and neodymium isotope distributions in the oceans. *Front. Mar. Sci.* 4, 426. <https://doi.org/10.3389/fmars.2017.00426>.
- Hamilton, S.K., Lewis, W.M., 1990. Basin morphology in relation to chemical and ecological characteristics of lakes on the Orinoco River floodplain, Venezuela. *Arch. Hydrobiol.* 119, 393–425.
- Hedges, J.L., Cowie, G.L., Richey, J.E., Quay, P.D., Benner, R., Strom, M., Forsberg, B.R., 1994. Origins and processing of organic matter in the Amazon River as indicated by carbohydrates and amino acids. *Limnol. Oceanogr.* 39, 743–761.
- Ingrí, J., Widerlund, A., Land, M., Gustafsson, Ö., Andersson, P., Öhlander, B., 2000. Temporal variations in the fractionation of the rare earth elements in a boreal river; the role of colloidal particles. *Chem. Geol.* 166, 23–45. [https://doi.org/10.1016/S0009-2541\(99\)00178-3](https://doi.org/10.1016/S0009-2541(99)00178-3).
- Johannesson, K.H., Zhou, X.P., 1999. Origin of middle rare earth element enrichments in acid waters of a Canadian high Arctic lake. *Geochem. Cosmochim. Acta* 63, 153–165. [https://doi.org/10.1016/S0016-7037\(98\)00291-9](https://doi.org/10.1016/S0016-7037(98)00291-9).
- Johannesson, K.H., Zhou, X., Guo, C., Stetzenbach, K.J., Hodge, V.F., 2000. Origin of rare earth element signatures in groundwater of circumneutral pH from southern Nevada and eastern California, USA. *Chem. Geol.* 164, 239–257. [https://doi.org/10.1016/S0009-2541\(99\)00152-7](https://doi.org/10.1016/S0009-2541(99)00152-7).
- Johannesson, K.H., Tang, J., Daniels, J.M., Bounds, W.J., Burdige, D.J., 2004. Rare earth element concentrations and speciation in organic-rich blackwaters of the Great Dismal Swamp, Virginia, USA. *Chem. Geol.* 209, 271–294. <https://doi.org/10.1016/j.chemgeo.2004.06.012>.
- Laraque, A., Castellanos, B., Steiger, J., López, J.L., Pandi, A., Rodríguez, M., Rosales, J., Adèle, G., Perez, J., Lagane, C., 2013. A comparison of the suspended and dissolved matter dynamics of two large inter-tropical rivers draining into the Atlantic Ocean: the Congo and the Orinoco. *Hydrol. Process.* 27, 2153–2170. <https://doi.org/10.1002/hyp.9776>.
- Laukert, G., Frank, M., Bauch, D., Hathorne, E.C., Rabe, B., von Appen, W.J., Wegner, C., Zieringer, M., Kassens, H., 2017. Ocean circulation and freshwater pathways in the Arctic Mediterranean based on a combined Nd isotope, REE and oxygen isotope section across Fram Strait. *Geochem. Cosmochim. Acta* 202, 285–309. <https://doi.org/10.1016/j.gca.2016.12.028>.
- Lewis, W.M., Saunders, J.F., 1989. Concentration and transport of dissolved and suspended substances in the Orinoco River. *Biogeochemistry* 7, 203–240. <https://doi.org/10.1007/BF00004218>.
- Li, M., Peng, C., Wang, M., Xue, W., Zhang, K., Wang, K., Shi, G., Zhu, Q., 2017. The carbon flux of global rivers: a re-evaluation of amount and spatial patterns. *Ecol. Indic.* 80, 40–51. <https://doi.org/10.1016/j.ecolind.2017.04.049>.
- Liu, C., Xu, M., Zhou, Z., Wang, G., Wu, C., Zhu, Y., Li, H., Ye, B., 2018. Magmatic history during late Carboniferous to early Permian in the north of the central Xing'an-Mongolia orogenic belt: a case study of the Houtoumiao pluton, Inner Mongolia. *Int. Geol. Rev.* 60, 1918–1939. <https://doi.org/10.1080/00206814.2017.1410731>.
- Liu, Q., Yang, X., 2018. Geochemical composition and provenance of aeolian sands in the Ordos Deserts, northern China. *Geomorphology* 318, 354–374. <https://doi.org/10.1016/j.geomorph.2018.06.017>.
- Lu, J., Huo, Y., Shen, Y., Hu, J., Ji, H., 2016. Effects of colloidal particle size on the geochemical characteristics of REE in the water in southern Jiangxi province, China. *Environ. Earth Sci.* 75, 1–17. <https://doi.org/10.1007/s12665-015-4870-0>.
- Machado-Allison, A., Chernoff, B., Bevilacqua, M., 2003. Introduction to the Caura River basin, Bolívar state, Venezuela. In: Chernoff, B., Machado-Allison, A., Riseng, K., Montambault, J.R. (Eds.), *A Biological Assessment of the Aquatic Ecosystems of the*

- Caura River Basin, Bolívar State, Venezuela. RAP Bulletin of Biological Assessment 28. Conservation International, Washington DC, USA, pp. 28–33.
- Matsunaga, T., Tsuduki, K., Yanase, N., Kritis-anuwat, R., Hanzawa, Y., Naganawa, H., 2015. Increase in rare earth element concentrations controlled by dissolved organic matter in river water during rainfall events in a temperate, small forested catchment. *J. Nucl. Sci. Technol.* 52, 514–529. <https://doi.org/10.1080/00223131.2014.961989>.
- Meade, R., Weibezahn, F., Lewis, W.M., Pérez, D., 1990. The Orinoco River as an ecosystem. In: Weibezahn, F.H., Alvarez, H., Lewis, W.M. (Eds.), *The Orinoco River as an Ecosystem*. Impresos Rubel CA, Caracas, pp. 55–79.
- Milliman, J.D., 2001. River inputs. In: Steele, J.H., Thorpe, S.A., Turekian, K.K. (Eds.), *Encyclopedia of Ocean Sciences*, second ed. Academic Press, San Diego, pp. 754–761.
- Minuzzi, O.R.R., Neto, A.C.B., Formoso, M.L.L., Andrade, S., Janasi, V.A., Flores, J.A., 2008. Rare earth element and yttrium geochemistry applied to the genetic study of cryolite ore at the Pitinga Mine (Amazon, Brazil). *An. Acad. Bras. Cienc.* 80, 719–733. <https://doi.org/10.1590/S0001-37652008000400012>.
- Moquet, J.S., Guyot, J.L., Crave, A., Viers, J., Filizola, N., Martinez, J.M., Oliveira, T.C., Sánchez, L.S.H., Lagane, C., Casimiro, W.S.L., Noriega, L., Pombosa, R., 2016. Amazon River dissolved load: temporal dynamics and annual budget from the Andes to the ocean. *Environ. Sci. Pollut. Res.* 23, 11405–11429. <https://doi.org/10.1007/s11356-015-5503-6>.
- Mora, A., Alfonso, J.A., Sánchez, L., Calzadilla, M., Silva, S., LaBrecque, J.J., Azócar, J.A., 2009. Temporal variability of selected dissolved elements in the lower Orinoco River, Venezuela. *Hydrol. Process.* 23, 476–485. <https://doi.org/10.1002/hyp.7159>.
- Mora, A., Baquero, J.C., Alfonso, J.A., Pisapia, D., Balza, L., 2010. The Apure River: geochemistry of major and selected trace elements in an Orinoco River tributary coming from the Andes. Venezuela. *Hydrol. Process.* 24, 3798–3810. <https://doi.org/10.1002/hyp.7801>.
- Mora, A., Laraque, A., Moreira-Turcq, P., Alfonso, J.A., 2014. Temporal variation and fluxes of dissolved and particulate organic carbon in the Apure, Caura and Orinoco rivers, Venezuela. *J. South Am. Earth Sci.* 54, 47–56. <https://doi.org/10.1016/j.jsames.2014.04.010>.
- Mora, A., Mahlknecht, J., Baquero, J.C., Laraque, A., Alfonso, J.A., Pisapia, D., Balza, L., 2017. Dynamics of dissolved major (Na, K, Ca, Mg, and Si) and trace (Al, Fe, Mn, Zn, Cu, and Cr) elements along the lower Orinoco River. *Hydrol. Process.* 31, 597–611. <https://doi.org/10.1002/hyp.11051>.
- Osborne, A.H., Haley, B.A., Hathorne, E.C., Plancherel, Y., Frank, M., 2015. Rare earth element distribution in Caribbean seawater: continental inputs versus lateral transport of distinct REE compositions in subsurface water masses. *Mar. Chem.* 177, 172–183. <https://doi.org/10.1016/j.marchem.2015.03.013>.
- Pang, H., Pan, B., Garzanti, E., Gao, H., Zhao, X., Chen, D., 2018. Mineralogy and geochemistry of modern Yellow River sediments: implications for weathering and provenance. *Chem. Geol.* 488, 76–86. <https://doi.org/10.1016/j.chemgeo.2018.04.010>.
- Piper, D.Z., Bau, M., 2013. Normalized rare earth elements in water, sediments, and wine: identifying sources and environmental redox conditions. *Am. J. Anal. Chem.* 4, 69–83. <https://doi.org/10.4236/ajac.2013.410A1009>.
- Pokrovsky, O.S., Schott, J., Dupré, B., 2006. Trace element fractionation and transport in boreal rivers and soil porewaters of permafrost-dominated basaltic terrain in Central Siberia. *Geochem. Cosmochim. Acta* 70, 3239–3260. <https://doi.org/10.1016/j.gca.2006.04.008>.
- Radomskaya, V.I., Radomskii, S.M., Kulik, E.N., Rogulina, L.I., Shumilova, L.P., Pavlova, L.M., 2017. Geochemical features of rare-earth elements in surface and subsurface waters in the field of the Albynokoe Gold-Bearing Placer, Amur oblast. *Water Resour.* 44, 284–296. <https://doi.org/10.1134/S00978078160600051>.
- Rengarajan, R., Sarin, M.M., 2004. Distribution of rare earth elements in the Yamuna and the Chambal rivers, India. *Geochem. J.* 38, 551–569. <https://doi.org/10.2343/geochemj.38.551>.
- Roddaz, M., Viers, J., Moreira-Turcq, P., Blondel, C., Sondag, F., Guyot, J.L., Moreira, L., 2014. Evidence for the control of the geochemistry of Amazonian floodplain sediments by stratification of suspended sediments in the Amazon. *Chem. Geol.* 387, 101–110. <https://doi.org/10.1016/j.chemgeo.2014.07.022>.
- Rosa, J.W.C., Rosa, J.W.C., Fuck, R.A., 2014. Geophysical structures and tectonic evolution of the southern Guyana shield, Brazil. *J. South Am. Earth Sci.* 52, 57–71. <https://doi.org/10.1016/j.jsames.2014.02.006>.
- Rousseau, T.C.C., Roddaz, M., Moquet, J.S., Handt Delgado, H., Calves, G., Bayon, G., 2019. Controls on the geochemistry of suspended sediments from large tropical South American rivers (Amazon, Orinoco and Maroni). *Chem. Geol.* 522, 38–54. <https://doi.org/10.1016/j.chemgeo.2019.05.027>.
- Rousseau, T.C.C., Sonke, J.E., Chmieleff, J., Van Beek, P., Souhaut, M., Boaventura, G., Seyler, P., Jeandel, C., 2015. Rapid neodymium release to marine waters from lithogenic sediments in the Amazon estuary. *Nat. Commun.* 6, 8592. <https://doi.org/10.1038/ncomms8592>.
- Ryu, J.S., Lee, K.S., Lee, S.G., Lee, D., Chang, H.W., 2007. Seasonal and spatial variations of rare earth elements in rainwaters, river waters and total suspended particles in air in South Korea. *J. Alloy. Comp.* 437, 344–350. <https://doi.org/10.1016/j.jallcom.2006.08.002>.
- Schulze, D.J., Canil, D., Channer, D.M.DeR., Kaminsky, F.V., 2006. Layered mantle structure beneath the western Guyana Shield, Venezuela: evidence from diamonds and xenocrysts in Guaniamo kimberlites. *Geochem. Cosmochim. Acta* 70, 192–205. <https://doi.org/10.1016/j.gca.2005.08.025>.
- Sheng, S., Xiuli, F., Guogang, L.I., Xiao, L.I.U., Xiao, X., Li, F., 2018. Change in sediment provenance near the current estuary of Yellow River since the Holocene transgression. *J. Ocean Univ. China* 17, 535–544. <https://doi.org/10.1007/s11802-018-3377-1>.
- Shiller, A.M., 2010. Dissolved rare earth elements in a seasonally snow-covered, alpine/subalpine watershed, Loch Vale, Colorado. *Geochem. Cosmochim. Acta* 74, 2040–2052. <https://doi.org/10.1016/j.gca.2010.01.019>.
- Shiller, A.M., 2002. Seasonality of dissolved rare earth elements in the lower Mississippi River. *Geochem. Geophys. Geosyst.* 3, 1–14. <https://doi.org/10.1029/2002GC000372>.
- Sholkovitz, E.R., 1992. Chemical evolution of rare earth elements: fractionation between colloidal and solution phases of filtered river waters. *Earth Planet. Sci. Lett.* 114, 77–84. [https://doi.org/10.1016/0012-821X\(92\)90152-L](https://doi.org/10.1016/0012-821X(92)90152-L).
- Sholkovitz, E.R., 1993. The geochemistry of rare earth elements in the Amazon River estuary. *Geochem. Cosmochim. Acta* 57, 2181–2190. [https://doi.org/10.1016/0016-7037\(93\)90559-F](https://doi.org/10.1016/0016-7037(93)90559-F).
- Sholkovitz, E.R., 1995. The aquatic chemistry of rare earth elements in rivers and estuaries. *Aquat. Geochem.* 1, 1–34. <https://doi.org/10.1007/BF01025229>.
- Silva León, G., 2005. La cuenca del río Orinoco: visión hidrográfica y balance hídrico. *Rev. Geogr. Venez.* 46, 75–108.
- Sivapragasam, C., Vanitha, S., Muttill, N., Suganya, K., Suji, S., Thamara Selvi, M., Selvi, R., Jeya Sudha, S., 2014. Monthly flow forecast for Mississippi River basin using artificial neural networks. *Neural Comput. Appl.* 24, 1785–1793. <https://doi.org/10.1007/s00521-013-1419-6>.
- Sklyarova, O.A., Sklyarov, E.V., Och, L., Pastukhov, M.V., Zagorulko, N.A., 2017. Rare earth elements in tributaries of lake Baikal (Siberia, Russia). *Appl. Geochem.* 82, 164–176. <https://doi.org/10.1016/j.apgeochem.2017.04.018>.
- Smith, C., Liu, X.M., 2018. Spatial and temporal distribution of rare earth elements in the Neuse River, North Carolina. *Chem. Geol.* 488, 34–43. <https://doi.org/10.1016/j.chemgeo.2018.04.003>.
- Song, H., Shin, W.J., Ryu, J.S., Shin, H.S., Chung, H., Lee, K.S., 2017. Anthropogenic rare earth elements and their spatial distributions in the Han River, South Korea. *Chemosphere* 172, 155–165. <https://doi.org/10.1016/j.chemosphere.2016.12.135>.
- Stallard, R.F., Koehnken, L., Johnsson, M.J., 1991. Weathering processes and the composition of inorganic material transported through the orinoco river system, Venezuela and Colombia. *Geoderma* 51, 133–165. [https://doi.org/10.1016/0016-7061\(91\)90069-6](https://doi.org/10.1016/0016-7061(91)90069-6).
- Stolpe, B., Guo, L., Shiller, A.M., 2013. Binding and transport of rare earth elements by organic and iron-rich nanocolloids in alaskan rivers, as revealed by field-flow fractionation and ICP-MS. *Geochem. Cosmochim. Acta* 106, 446–462. <https://doi.org/10.1016/j.gca.2012.12.033>.
- Su, N., Yang, S., Guo, Y., Yue, W., Wang, X., Yin, P., Huang, X., 2017. Revisit of rare earth element fractionation during chemical weathering and river sediment transport. *Geochem. Geophys. Geosyst.* 18, 935–955. <https://doi.org/10.1002/2016GC006659>.
- Sultan, K., Shazili, N.A., 2009. Rare earth elements in tropical surface water, soil and sediments of the Terengganu River Basin, Malaysia. *J. Rare Earths* 27, 1072–1078. [https://doi.org/10.1016/S1002-0721\(08\)60391-9](https://doi.org/10.1016/S1002-0721(08)60391-9).
- Tachikawa, K., 2003. Neodymium budget in the modern ocean and paleo-oceanographic implications. *J. Geophys. Res.* 108, 3254. <https://doi.org/10.1029/1999JC000285>.
- Tachikawa, K., Arsouze, T., Bayon, G., Bory, A., Colin, C., Dutay, J.C., Frank, N., Giraud, X., Gourelan, A.T., Jeandel, C., Lacan, F., Meynadier, L., Montagna, P., Piotrowski, A.M., Plancherel, Y., Pucéat, E., Roy-Barman, M., Waelbroeck, C., 2017. The large-scale evolution of neodymium isotopic composition in the global modern and Holocene ocean revealed from seawater and archive data. *Chem. Geol.* 457, 131–148. <https://doi.org/10.1016/j.chemgeo.2017.03.018>.
- Taylor, S.R., McLennan, S., 1985. *The Continental Crust: its Composition and Evolution*. Blackwell Scientific Publications, Oxford, p. 312.
- Taylor, S.R., McLennan, S.M., Armstrong, R.L., Tarney, J., 1981. The composition and evolution of the continental crust: rare earth element evidence from Sedimentary Rocks. *Philos. T. R. Soc. A* 301 (1461), 381–399. <https://doi.org/10.1098/rsta.1981.0119>.
- Uchida, S., Tagami, K., Tabei, K., Hirai, I., 2006. Concentrations of REEs, Th and U in river waters collected in Japan. *J. Alloy. Comp.* 408–412, 525–528. <https://doi.org/10.1016/j.jallcom.2004.12.104>.
- Viers, J., Barroux, G., Pinelli, M., Seyler, P., Oliva, P., Dupré, B., Boaventura, G.R., 2005. The influence of the Amazonian floodplain ecosystems on the trace element dynamics of the Amazon River mainstem (Brazil). *Sci. Total Environ.* 339, 219–232. <https://doi.org/10.1016/j.scitotenv.2004.07.034>.
- Warne, A.G., Meade, R.H., White, W.A., Guevara, E.H., Gibeau, J., Smyth, R.C., Aslan, A., Tremblay, T., 2002. Regional controls on geomorphology, hydrology, and ecosystem integrity in the Orinoco Delta, Venezuela. *Geomorphology* 44, 273–307. [https://doi.org/10.1016/S0169-555X\(01\)00179-9](https://doi.org/10.1016/S0169-555X(01)00179-9).
- Weibezahn, F.H., 1990. Water chemistry and suspended solids in the upper and middle Orinoco River. In: Weibezahn, F.H., Alvarez, H., Lewis, W.M. (Eds.), *The Orinoco River as an Ecosystem*. Impresos Rubel CA, Caracas, pp. 151–210.
- Xu, Z., Han, G., 2009. Rare earth elements (REE) of dissolved and suspended loads in the Xijiang River, South China. *Appl. Geochem.* 24, 1803–1816. <https://doi.org/10.1016/j.apgeochem.2009.06.001>.
- Yeghicheyan, D., Bossy, C., Bouhnik Le Coz, M., Douchet, C., Granier, G., Heimburger, A., Lacan, F., Lanzaova, A., Rousseau, T.C.C., Seidel, J.L., Tharaud, M., Candaudap, F., Chmieleff, J., Cloquet, C., Delpoux, S., Labatut, M., Losno, R., Pradoux, C., Sivry, Y., Sonke, J.E., 2013. A compilation of silicon, rare earth element and twenty-one other trace element concentrations in the natural river water reference material SLRS-5 (NRC-CNRC). *Geostand. Geoanal. Res.* 37, 449–467. <https://doi.org/10.1111/j.1751-908X.2013.00232.x>.
- Zhang, C., 1998. Geochemistry of rare earth elements in the mainstream of the Yangtze River, China. *Appl. Geochem.* 13, 451–462. [https://doi.org/10.1016/S0883-2927\(97\)00079-6](https://doi.org/10.1016/S0883-2927(97)00079-6).